Comparison of Candidate Secondary Electron Emission Materials

Z. Insepov*, V. Ivanov[+], and H. Frisch[§]

*Mathematics and Computer Science Division, Argonne National Laboratory, Argonne, Illinois
[+]Muons Inc., Batavia, Illinois
[§]High-Energy Physics Division, Argonne National Laboratory, Argonne, Illinois

ABSTRACT

We have developed a theoretical method for calculating secondary electron emission (SEE) yields. The method uses Monte Carlo simulation, empirical theories, and close comparison to experiment, in order to parameterize the SEE yields of highly emissive materials. We have successfully applied this method to bulk Al_2O_3, a highly emissive material for microchannel plates, as well as to thinly deposited films of Al_2O_3. The simulation results will be used in the selection of emissive and resistive materials for the deposition and characterization experiments that will be conducted by a large-area fast detector project at Argonne National Laboratory.

1. INTRODUCTION

Theoretical studies of secondary electron emission yields are important for developing computational tools capable of calculating the secondary electron (SE) emission yields for a range of high-SE-yield engineering materials (emissive materials) that can be used in particle detectors for high-energy physics, such as Cherenkov, neutrino detectors, and astroparticle detectors [1,2]. Secondary electrons also play a significant role in visualizing micron-sized patterns in scanning electron microscopy (SEM); theory and simulation of SE emission is therefore a large part of SEM development [3-13].

SE emission of surfaces exposed to high-gradient electromagnetic fields is one of the factors of the multipacting effect that can significantly degrade the performance of particle accelerators. Therefore, reducing the SE yield is a key issue for the development of future accelerators [14]. Fusion devices are also susceptible to SE emission, which can cause surface breakdown at high electric gradients [15].

The goal of this work is to develop a parameterized set of the SE-yield dependencies on two variables, the primary electron energy (E_{PE}) and the angle of incident electrons (θ), for materials of interests in the large-area fast detector development project at Argonne National Laboratory. This parameterization can be done by using results obtained from Monte Carlo calculations with existing codes [3-7] modified to meet the needs of microchannel plate (MCP) developments, as well as by using the results of empirical SE-yield models [16-19]. Modification of the Monte Carlo codes will be necessary to address and include into the database new, highly emissive materials such as MgO, ZnO, and Al_2O_3, which are important for MCP development [5-7]. We will also need to study resistive materials that will be used for coating the MCP pores. The method will be verified with experimental data obtained in the literature and with new data measured specifically for the large-area fast detector project. The calculated yields will also be used as input files for macroscopic MCP gain and transient time calculation codes for computing electron trajectories inside MCPs of various types, such as chevron and funnel. Feedback from

the gain code will then be used to improve the materials data and will stimulate further search for the best MCP emissive and resistive materials.

2. SECONDARY ELECTRON EMISSION YIELDS

Secondary electron emission is an important tool for surface microanalysis in various research, science, and industrial areas. Primary electron collisions with the surface of a target generate emissions of various types of secondary electrons [10]:

- "True" secondary electrons having kinetic energies < 50 eV (depending on the material, the most probable energy of SE is about 1-3 eV, and the average energy is between 4 and 5 eV [10]).
- Auger electrons.
- Elastically reflected backscattered (BS) electrons, having energies 50 eV < E < E_{PE} , where E_{PE} is the primary electron energy.

The following coefficients are defined according to these processes: SE1 is the number of secondary electrons emitted by primary electrons within the escape range, and SE2 is the number of secondary electrons emitted by the backscattered ones on their way back to the surface. SE2 = $\beta\eta$*SE1, where η is the backscattered yield and β is the efficiency with which backscattered electrons generate the secondary electrons. The total number of SE electrons per primary electron, δ, is the number of electrons emitted with higher energies. The total yield is SE1(1+ $\beta\eta$).

2.1. Energy Dependence

Several researchers have developed semi-empirical theories [5-11]. Such theories are helpful in calibrating Monte Carlo simulations, which are the main tool for obtaining the SE yield for various materials at different energies and incident angles of primary electrons.

The SE yield can be written in the following form [10]:

$$\delta = \int n(x, E_{PE}) f(x) dx, \qquad (1)$$

where $n(x,E_{PE})$ is the number of secondary electrons produced at a distance x from the surface by a primary electron with the energy of E_{PE}, and $f(x)$ is the probability that the secondary electrons will escape from the surface.

It is assumed that n is proportional to the average energy loss in the target:

$$n(x, E_{PE}) = -\frac{1}{\varepsilon}\frac{dE}{dx}, \qquad (2)$$

where ε is the energy per secondary electron emitted at a distance x from the surface. The probability of the secondary electron traveling to the surface and escaping from the surface is as follows:

$$f(x) = Be^{-x/\lambda}, B < 1, \qquad (3)$$

where λ is the mean electron escape depth [7,9].

Young [11] showed that the electron energy loss inside the target is approximately constant:

$$-\frac{dE}{dx} = E_{PE}/R, \qquad (4)$$

By using the above formulas, we can get a combined SE yield as follows:

$$\delta = \int_0^{\infty} \frac{B}{\varepsilon} \frac{E_{PE}}{R} e^{-x/\lambda} dx, \tag{5}$$

$$\delta(E_{PE}) = B \frac{E_{PE}}{\varepsilon} \frac{\lambda}{R} \left(1 - e^{-R/\lambda}\right). \tag{6}$$

The electron ranges R in Al_2O_3 were measured by Young [11], who proposed a formula that was in close agreement with Bethe's theory prediction at low electron energies [10]:

$$R \Big/ [mg/cm^2] = 0.0115 \left(\frac{E_{PE}}{[keV]} \right)^{1.35}. \tag{7}$$

If δ_m and E^m are the yield and energy at maximum, respectively, the reduced yield δ/δ_m is independent of the materials constants B, ε, and ρ. This is called a universal curve:

$$\frac{\delta}{\delta_m} = 1.11 \left(\frac{E_{PE}}{E_{PE}^m} \right)^{-0.35} \left(1 - e^{-2.3\left(\frac{E_{PE}}{E_{PE}^m}\right)^{1.35}} \right), \tag{8}$$

where E and E^m are the primary electron energies at maximum.

Lin and Joy [6] calculated the ion ranges by a slightly different formula:

$$R = \frac{B}{\rho} (E_{PE})^{1.67}.$$

Here B = 76 nm, E_{PE} is in keV, and ρ is in grams per cubic centimeter, giving a different final expression:

$$\frac{\delta}{\delta_m} = 1.28 \left(\frac{E_{PE}}{E_{PE}^m} \right)^{-0.67} \left(1 - e^{-1.614\left(\frac{E_{PE}}{E_{PE}^m}\right)^{1.67}} \right), \tag{9}$$

Formulas (8) and (9) are usually referred to as the "universal law of SE yield" [5-10]. They provide a valuable calibration tool for developing Monte Carlo codes for SE studies. Specifically, if no reliable theoretical or experimental data for δ_m and E_m exist, such data can be obtained from Monte Carlo simulations and be used to quantify the SE yields for new materials by using the "universal law." Such extensive analysis has been done by Lin and Joy [6], who obtained the universal law parameters for 44 elements with Z = 3-83.

2.2. Monte Carlo Codes

Several researchers have developed Monte Carlo codes based on the above theory that are applicable to low-energy SE-yield calculations [3-7]. The Rutherford cross-section for elastic electron scattering of low-E electrons and high-Z materials was replaced by Mott's cross-section, which was tabulated for the electron energies in the range of 1-100 keV [3]. The inelastic energy loss of electrons is usually approximated by Bethe's equation:

$$\frac{dE}{dS} = -78{,}500 * \frac{Z}{AE} * \log_e \left(\frac{1.166E}{J} \right), \tag{10}$$

where dE/dS is the stopping power of the target, E is the energy of the primary electrons, Z is the atomic number, A is the atomic weight, and S is the product of the density ρ [g/cm^3] and the distance traveled by the electron. J is the mean ionization energy of the target material and is

obtained from experiment. This variable includes all inelastic energy mechanisms and allows researchers to study the energy loss in a compact and simple way by using the Bethe equation. The experimental value of J for Al_2O_3 is 145 eV [5,7]. There are no measured values of J for ZnO and MgO.

Berger and Seltzer [7] proposed an empirical formula applicable to high-energy electrons as follows:

$$J = \left[9.76\,Z + \frac{58.5}{Z^{0.19}} \right] * 10^{-3}, (\text{keV}). \qquad (11)$$

For compound materials (e.g., ZnO), an averaged value for atomic number can be used:

$$Z_{av} = \left(1 * Z_{Zn} + 1 * Z_O\right) \Big/ 2, \qquad (12)$$

which gives J_{ZnO}=219 eV and J_{MgO} = 135 eV.

The Bethe approximation (10) was improved by Seiler [10] for low-energy electrons.

Two important simulation parameters in the MC model shown in eq. (6). One is ε, the average energy for producing secondary electron, and the other is the escape depth λ. These two parameters have a significant impact on the simulation result. We used ε = 20 eV for Al_2O_3 [8]. The escape depth λ of insulators can be relatively large compared to that of metal surfaces, a direct effect of the small absorption coefficient of low-energy electrons in insulators because of the large energy band gap (e.g., E_g = 8 eV in Al_2O_3). Kanaya et al. [9] proposed a theoretical model for calculating the escape depth for a range of insulators and alkaline materials. Based on this analysis, the escape length can be chosen as λ = 60Å for Al_2O_3. This value was also suggested by Joy [8].

2.3. Angular Dependence

SE yield at high primary electron energies E_{PE} > 1 MeV increases as the angle of incidence θ relative to the normal increases (θ < 80°), with the exception of grazing angles. This is caused by a decrease of λ:

$$\delta(\theta) = \delta_0 (\cos\theta)^{-n}, \qquad (13)$$

The power exponent n = 1 is applicable for the target materials with Z approximately equal to 30 [7]. For light elements $n \approx 1.3$, and for heavy elements $n \approx 0.8$. This law is not applicable to the electrons with low and intermediate energies typical for MCP development.

Ohya and Mori [13] have studied the SE yield at lower energies, ~ 100 eV. They found that eq. (13) can fail at low energies.

3. EMPIRICAL MODELS

Ito et al. [16] proposed the following empirical model for calculating the average number of emitted electrons:

$$\delta(\theta_i, \varepsilon_i) = 4\nu_i \cdot \delta_m(\theta_i) \Big/ \left\{ \varepsilon_m(\theta_i) \cdot \left(1 + \varepsilon_i / \varepsilon_m(\theta_i)\right)^2 \right\}, \qquad (14)$$

where θ_i and ε_i are incident angle and energy of the electron hitting the target's surface, respectively, and $\delta_m(\theta i)$ and $\varepsilon_m(\theta i)$ are the maximum yield and the incident energy for the maximum yield, respectively:

$$\delta_m(\theta_i) = \delta_{m0} \cdot \exp[\alpha(1-\cos\theta_i)],$$
$$v_m(\theta_i) = v_{m0} \Big/ \sqrt{\cos\theta_i}. \qquad (15)$$

Here δ_{m0} is the maximum yield corresponding to the electrons with incident angle normal to the surface, v_{m0} is the incident energy for the maximum yield, and α is the material constant.

Guest et al. [17] developed another empirical SE-yield model that contains eq. (15) as correct experimental input data. The reduced SE yield is obtained by the following equation,

$$\delta \Big/ \delta_m(0) = \left(\frac{\varepsilon}{\varepsilon_m}\sqrt{\cos\theta}\right)^{\beta} \exp[\alpha(1-\cos\theta)] + \beta\left(1-\frac{\varepsilon}{\varepsilon_m}\sqrt{\cos\theta}\right), \qquad (16)$$

where β is the adjustable parameter chosen to fit the experimental SE yields at normal electron incidence.

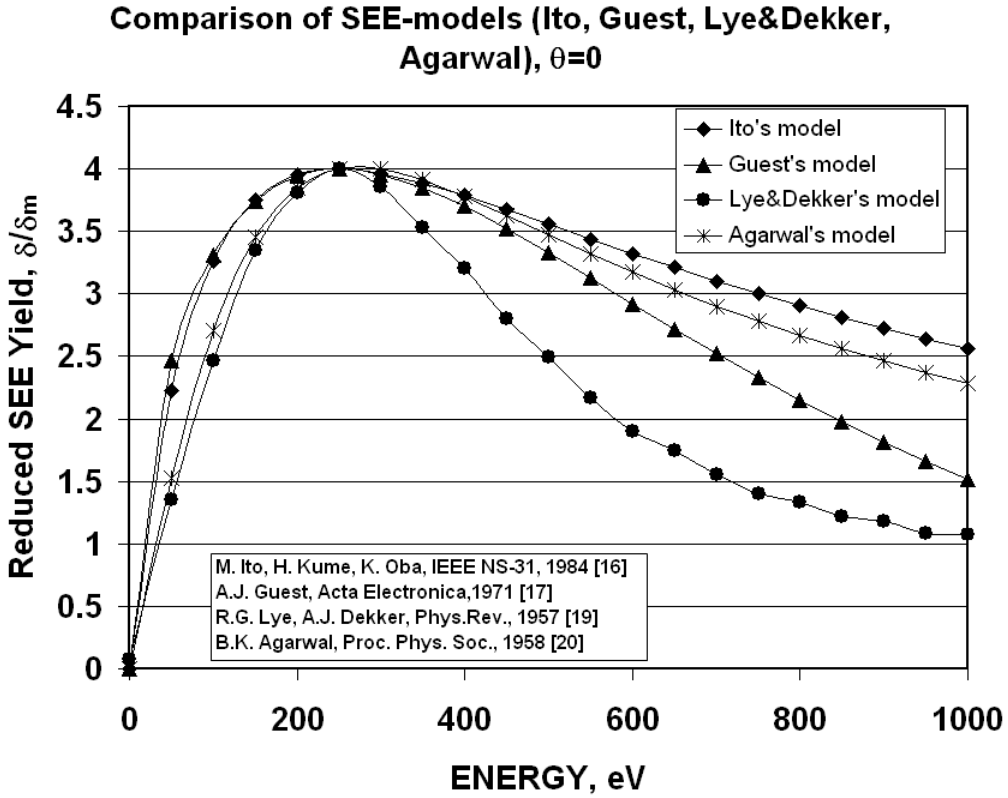

Fig. 1. Comparison of the empirical models of the secondary electron emission yields in reduced form at normal incidence. The maximum yields and the incident energies at maximum for all models were chosen to be the same as for Ito's model: $\delta_m = 4$, $\varepsilon_m = 250$ eV.

Baroody [18] and Lye and Dekker [19] proposed a model that can be reduced to the following simple form:

$$\delta/\delta_m = \frac{1}{F(0.92)} F(0.92\, E_0/E_{0m}),$$
$$F(r) = \exp(-r^2)\int_0^r \exp(y^2)dy. \tag{17}$$

Agarwal [20] proposed a new formula that improves the high-energy behavior of the Lye-Dekker and Ito's models and can be represented via the following formula:

$$\delta/\delta_m = \frac{2(E_0/E_{0m})}{1+(E_0/E_{0m})^{1.85(2Z/A)}}, \tag{18}$$

where Z and A are the atomic number and atomic weight.

These four models are compared in Fig. 1.

4. SIMULATION RESULTS

Figures 2-4 show the energy and angular dependences of the SE yield of electrons colliding with a Al_2O_3 surface at incident angles $0° \le \theta_i \le 89°$

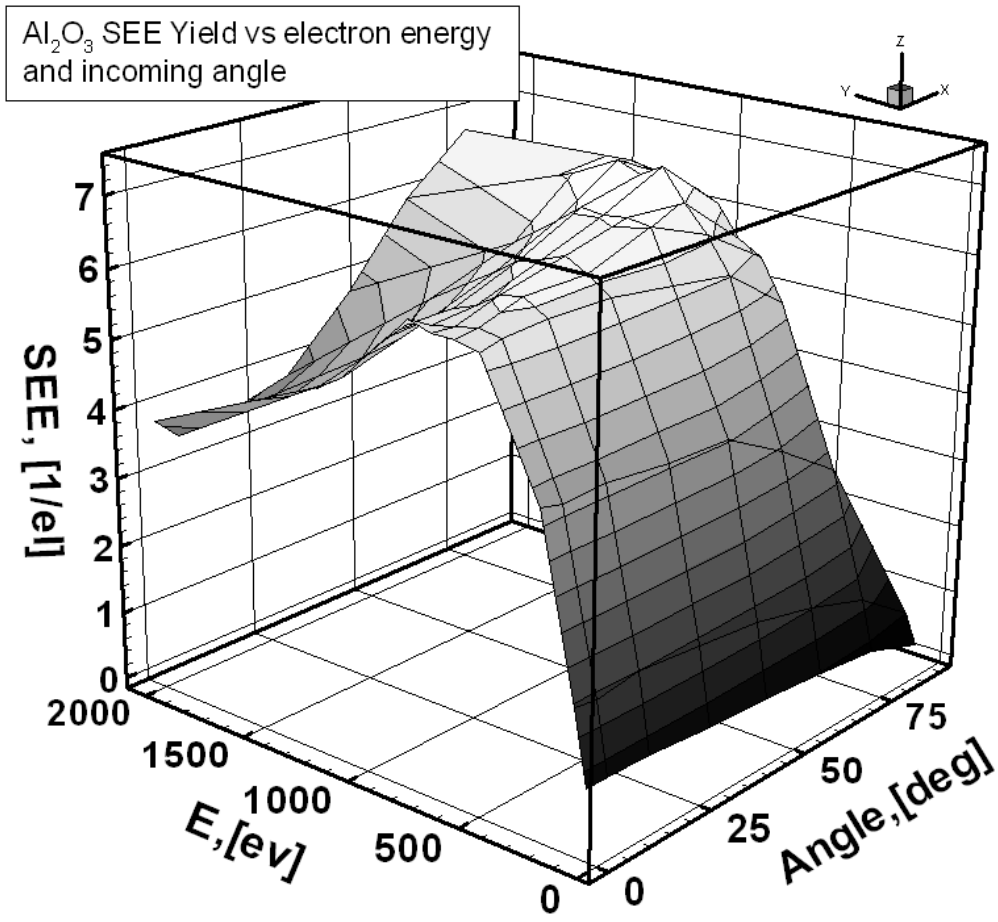

Fig. 2. SE yield generated by primary electrons with energies of E =50-2000 eV and incident angles in the range of $0° \le \theta_i \le 89°$.

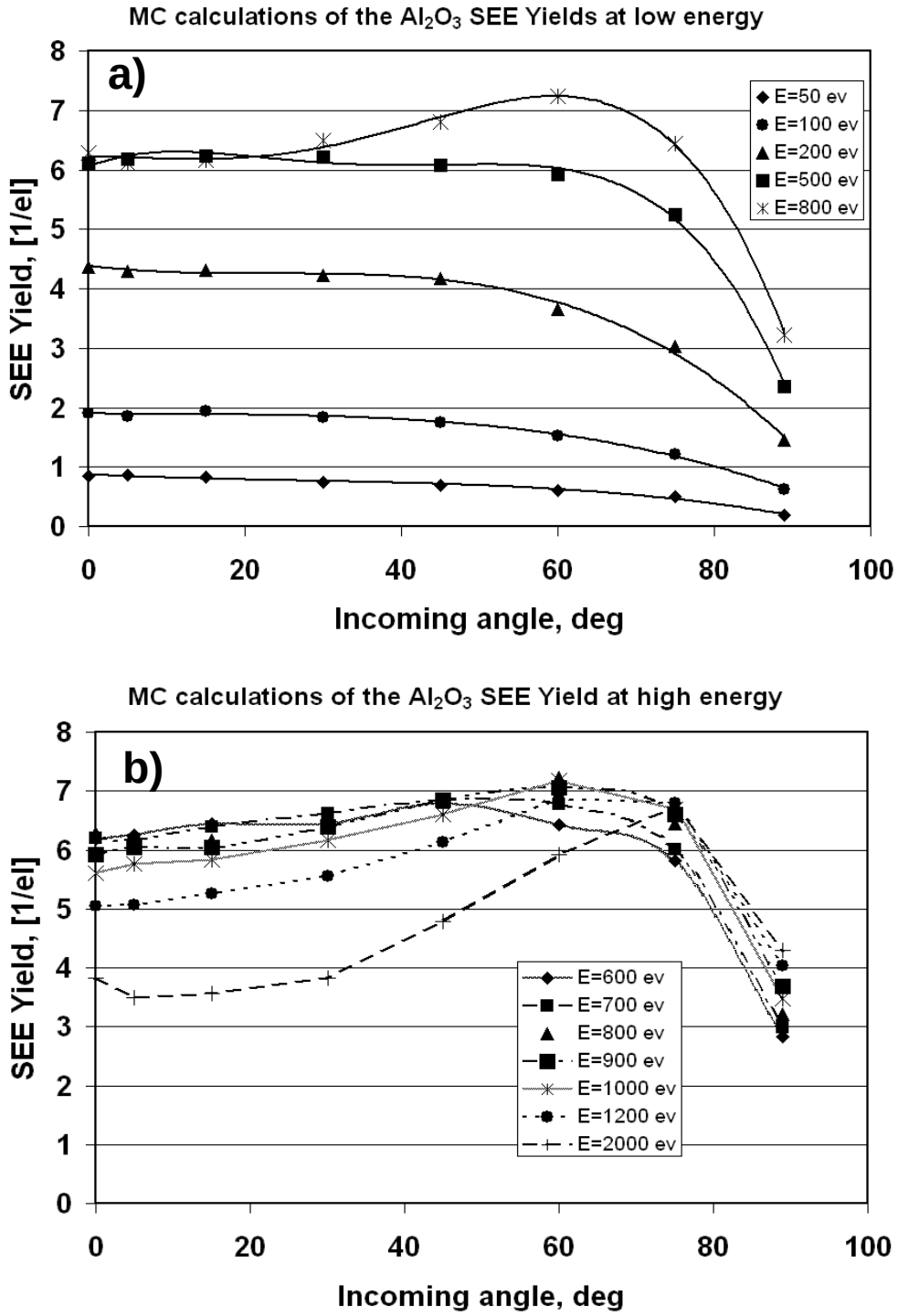

Fig. 3. SE yields generated by electrons colliding with a 5 nm Al_2O_3 thin film, with energies E = 50-2000 eV and incident angles in interval $0° \leq \theta_i \leq 89°$: (a) E = 50-800 eV, (b) E = 600-2000 eV.

5. COMPARISON WITH EXPERIMENT

Since the charging of highly resistive ceramics gives incorrect SE-yield results, it is important to compare the experimental measurements with the Al_2O_3 emission rates obtained by Monte Carlo simulations. Dawson measured SE yields of an Al_2O_3 surface by using a pulsed technique that guaranteed that if the surface was charged, it could be replenished by a very low energy electron shower between the two pulses [21]. Figure 4 shows close agreement between experiment and simulation, which is important because mathematical difficulties have resulted in almost no theory for low-energy electron emissions.

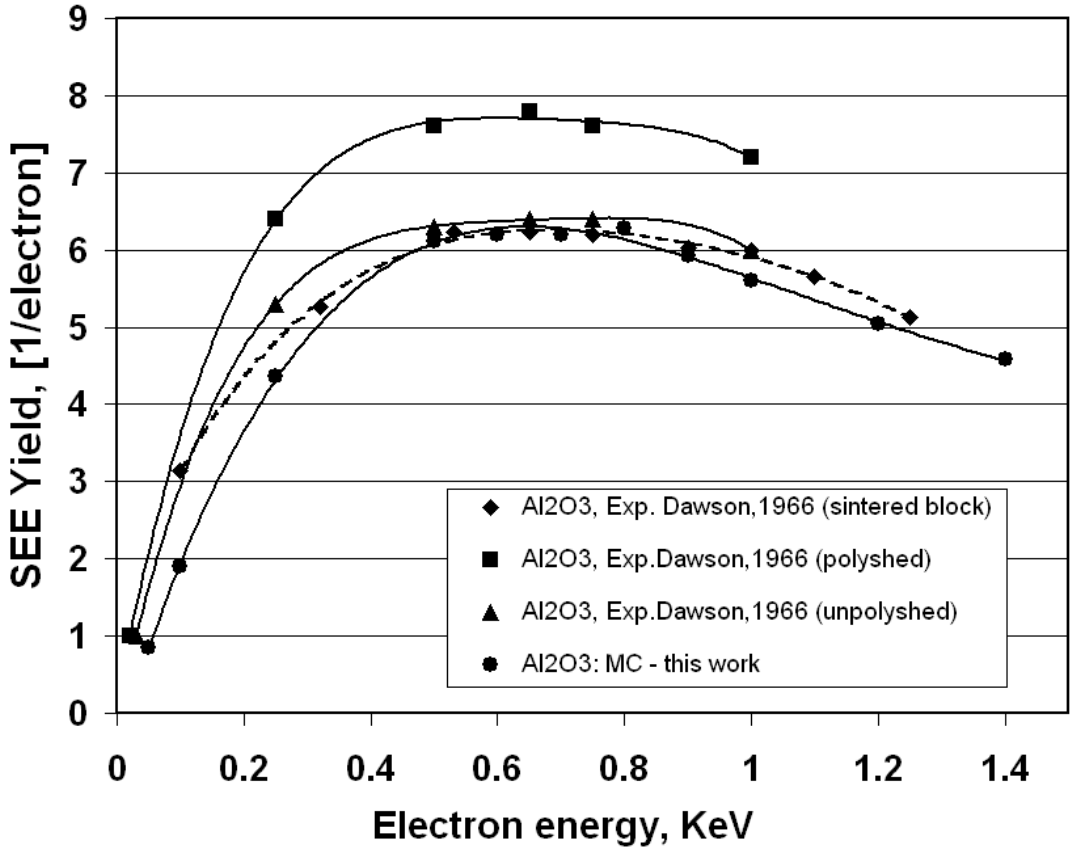

Fig. 4. Comparison of the Monte Carlo simulation results for Al_2O_3 with experimental data obtained by Dawson [21] for polished (pink), unpolished (dark blue), and sintered surface (green) curves and symbols. Our simulation is shown as cyan symbols and blue curve.

The Monte Carlo simulation did not use any experimental data; the important parameters were obtained from empirical theories. However, since these theories are often not applicable to low-energy electrons typical of MCP operation, we can assume that the escape length for the electrons in Al_2O_3 is an adjustable parameter, rather than calculated from theory. Other parameters of Al_2O_3 that were used to generate the SE yield shown in Figs. 2-4 are as follows: $Z_{av} = 10$; $A_{av} = 20.39$, where "av" means averaging for compound material; and $\rho = 3.9$ g/cm^3.

6. Summary

MCP gain and transient time simulations are closely related to the SE yields calculated in this paper. The SE yields are expressed as a parameterized function of two variables: primary electron energy and incident angle. In this paper, we have presented an approach that combines Monte Carlo simulation of the secondary electron emission with empirical SE theories and experiment. We showed that this approach gives a close agreement for Al_2O_3, for which extensive experimental data and theory exist for obtaining important simulation parameters such as energy and escape length of secondary electrons. This parameterization work is ongoing, and the results will be published elsewhere.

The theory of SE yields at low electron energies is limited. Therefore, the simulations and comparison to experiment for such yields are important. We plan to calculate the SE yields for those candidate materials having high emissive properties, such as Al_2O_3, ZnO, mixture of Al_2O_3+ZnO, and MgO. We will also simulate multilayer structures, in order to increase the yield. In addition, we will calculate SE yields of rough surfaces [22] and to compare our results with a probability method developed by Furman and Pivi [23].

Acknowledgment

This work was supported by the U.S. Department of Energy, under Contract DE-AC02-06CH11357.

References

[1] E. Nappi, Advances in the photodetection technologies for Cherenkov imaging applications, Nucl. Instr. Meth. A 604 (2009) 190-192.

[2] S.M. Bradbury, R. Mirzoyan, J. Gebauer, E. Feigl, E. Lorenz, Test of the new hybrid INTEVAC intensified photocell for the use in air Cherenkov telescopes, Nucl. Instr. Meth. A387 (1997) 45-49.

[3] L. Reimer, D. Stelter, FORTRAN 77 Monte-Carlo program for minicomputers using Mott cross-section, Scanning 8 (1986) 265-277.

[4] S. Ishimura, M. Aramata, R. Shimizu, Monte-Carlo calculation approach to quantitative Auger electron spectroscopy, J. Appl. Phys. 51 (1980) 2853-2860.

[5] D.C. Joy, Monte Carlo modeling for electron microscopy and microanalysis, Oxford Univ. Press, 1995.

[6] Y. Lin, D.C. Joy, A new examination of secondary electron yield data, Surf. Interface Anal. 37 (2005) pp. 895–900.

[7] D.C. Joy, A model for calculating secondary and backscattering electron yields, J. of Microscopy, 147 (1987) 51–64.

[8] D.C. Joy, private communication, 2009.

[9] K. Kanaya, S. Ono, F. Ishigaki, Secondary electron emission from insulators, J. Phys. D 11 (1978) 2425-2437.

[10] H. Seiler, Secondary electron emission in the scanning electron microscope, J. Appl. Phys. 54 (1983) R1-R18.

[11] J.R. Young, Penetration of electrons in Al_2O_3-films, Phys. Rev. 103 (1956) 292-293.

[12] R.O. Lane, D.I. Zaffarano, Transmission of 0-40 keV electrons by thin films with application to beta-ray spectroscopy, Phys. Rev. 94 (1954) 960-964.

[13] K. Ohya, I. Mori, Influence of backscattered particles on angular dependence of secondary electron emission from Copper, J. Phys. Soc. Jpn. 59 (1990) 1506-1517.

[14] V. Baglin, J. Bojko, O. Gröbner, B. Henrist, N. Hilleret, C. Scheuerlein, M. Taborelli, The secondary electron yield of technical materials and its variation with surface treatments, Proc. of EPAC 2000, pp. 217-221, Vienna, Austria.

[15] K. Jakubka, B. Jüttner, On the influence of surface conditions on initiation and spot types of unipolar arcs in a Tokamak, J. Nucl. Mater. 102 (1981) 259-266.

[16] M. Ito, H. Kume, K. Oba, Computer analysis of the timing properties in micro channel plate photomultiplier tubes, IEEE Trans. NS-31 (1984) 408-412.

[17] A.J. Guest, A computer model of channel multiplier plate performance, Acta Electronica, 14 (1971) pp.79-97.

[18] M. Baroody, A theory of secondary emission, Phys. Rev. 78 (1950) 780-787.

[19] R.G. Lye, A.J. Dekker, Theory of secondary emission, Phys. Rev. 107 (1957) 977-981.

[20] B.K. Agarwal, Variation of secondary emission with primary electron energy, Proc. Phys. Soc. 71 (1958) 851-852.

[21] P.H. Dawson, Secondary electron emission yields of some ceramics, J. Appl. Phys. 37 (1966) 3644-3665.

[22] J. Kawata, K. Ohya, K. Nishimura, Simulation of secondary electron emission from rough surfaces, J. Nucl. Mater. 220-222 (1995) 997-1000.

[23] M. A. Furman, M.T. F. Pivi, Probabilistic model for the simulation of secondary electron emission, Phys. Rev. ST AB 5, 124404 (2002).

The submitted manuscript has been created by UChicago Argonne, LLC, Operator of Argonne National Laboratory ("Argonne"). Argonne, a U.S. Department of Energy Office of Science laboratory, is operated under Contract No. DE-AC02-06CH11357. The U.S. Government retains for itself, and others acting on its behalf, a paid-up nonexclusive, irrevocable worldwide license in said article to reproduce, prepare derivative works, distribute copies to the public, and perform publicly and display publicly, by or on behalf of the Government.